

Improvement Tolerant Control of Shunt Active Power Filter Under Unbalanced Loads

K. Frifita, M. Boussak, *Senior Member IEEE*, A. Naamane, N. M'Sirdi

Abstract—This paper deals with a tow robust configurations of a shunt active power filter (SAPF) to optimize the energy transfer in unbalanced load conditions. These structures are designed to minimize the real-time computation requirements. To control this SAPF system, an instantaneous active and reactive power (p - q) method for harmonic detection and a phase locked loop (PLL) control strategy have been used and have been simulated by using Matlab/Simulink. These simulation results show the effectiveness of the proposed method.

Keywords—Shunt active power filter (SAPF), instantaneous active and reactive power method, phase locked loop (PLL) control, unbalance load tolerant controls.

i_{f1}, i_{f2}, i_{f3}	Currents injected by SAPF
i_{c1}, i_{c2}, i_{c3}	Load currents
i_{sn}	Neutral current
K_1, K_2	PLL filter continuous parameters
ω_0	Angular frequency of PLL reference signal
VCO	Voltage controlled oscillator of PLL control
V_1, V_2, V_3	Output voltages inverter
U_{dc0}	Average value of U_{dc}
$U_{dc\max}$	Maximum value of U_{dc}
$U_{dc\min}$	Minimum value of U_{dc}

NOMENCLATURE

R_{f1}, R_{f2}, R_{f3}	Filter resistances
L_{f1}, L_{f2}, L_{f3}	Filter inductances
L_{fn}	Neutral inductance
C	Capacitor
E	Energy stored in C
U_{dc}	Continuous voltage inverter
V_{r1}, V_{r2}, V_{r3}	Grid voltages
V_r	RMS voltage grid
V_α, V_β	Stationary reference frame grid voltages
p	Instantaneous active power
q	Instantaneous reactive power
p_o	Zero-sequence instantaneous active power
i_α, i_β, i_o	Stationary reference frame grid currents
i_{s1}, i_{s2}, i_{s3}	Grid currents
\tilde{p}	Alternating value of instantaneous active power
\bar{p}	Mean value of the instantaneous active power
i_{h1}, i_{h2}, i_{h3}	Inverter reference currents
V_f	IGBT continuous voltage source
R_{on}	Turn-on IGBT resistance
L_{on}	Turn-on IGBT inductance

I. INTRODUCTION

NOWADAYS the increasing usage of the power electronic converters creates many problems in the electricity grid. In fact, these pollution sources absorb non-sinusoidal, and consume reactive power with generation of the harmonic currents in electric system [1]–[4]. This harmonics generation represents the permanent disturbances affecting the waveform of the grid current. This problem results in power factor (PF) degradation and generates alternating voltages and currents which have a different frequency than the fundamental. Indeed, those harmonics represent the principal causes of degradation and fall of the power switches [1],[3].

In electric grid distribution some standards such as ISO - 1540 and DO-160F have been used to keep limits on harmonic current components [1],[3],[5]. Using these standards, many solutions are proposed to solve or minimize the harmonic problems. The first solution is based on passive filters that are composed of inductive and capacitive (LC) elements. But this solution has many drawbacks, mainly with the unbalanced nonlinear loads [6].

To overcome these problems for compensating the harmonic distortion and unbalance, the shunt active power filter (SAPF) is applied. The global principle of this filter is to balance the electric grid distribution (50 Hz) based on injection of a compensating current in phase opposition to the harmonic currents produced by nonlinear load [1]–[3].

Recently, many solutions are proposed to eliminate the harmonic problem with SAPF under balanced and/or unbalanced load [6]–[9]. In this topic, a comprehensive review of performance and implementation of the SAPF is presented in [1] and [2] where a comparison between many structure and control strategies is presented. The authors of [1],[6],[7] studied the case of unbalanced load and proposed solutions to reduce the current of neutral and raise the yield

K. Frifita, A. Naamane and N. M'Sirdi are with Aix–Marseille Université (AMU)–Laboratoire des Sciences de l'Information et des Systèmes (LSIS) – UMR CNRS 7296 – Domaine Univ. de Saint Jérôme – case LSIS– Avenue Escadrille Normandie Niemen– 13397Marseille–France:(e-mail: khaled.frifita@lsis.org, aziz.naamane@lsis.org, nacer.msirdi@lsis.org).

M. Boussak is with Ecole Centrale Marseille (ECM) –Laboratoire des Sciences de l'Information et des Systèmes (LSIS) – UMR CNRS 7296 – 38 Rue Frédéric-Joliot Curie –13451 Marseille Cedex 20 – France, (e-mail: mohamed.boussak@centrale-marseille.fr).

of SAPF. This solution based on a modification of the SAPF control strategy to generate new gating signals or/and the global structural of the SAPF.

In the same case (unbalanced load) [8], [9] used two structures to make a high performance SAPF. Their first structure is based on a three leg power inverter where a connection between the neutral wire and the midpoint of continuous voltage is assured if an unbalanced problem is detected. But the other structure is based on a four legs inverter bridge. To control the SAPF in the best condition and generate the reference currents, many control methods has been proposed [2], [3]:

- Instantaneous reactive power ($p-q$) method [10]–[12].
- Modified Fourier transforms technique [2], [15].
- Synchronous reference frame ($d-q$) method [13], etc.

These methods are related to other generation gating signal techniques. In [3] and [16] a hysteresis comparator technique is developed because because it is esier to implement, but causing high losses on variable switching frequency [1], [2].

This paper is mainly devoted to the SAPF control under unbalanced load tolerant structures organized as follows. In section II, we present the SAPF structure and its control applied to a balanced and unbalanced loads. In this section two unbalanced tolerant controls are presented with its unbalanced detection method. To synchronize the current and voltage phases, a PLL strategy is used taking into account the stability of the studied system. These tolerant structures use the pulse width modulation (PWM) technique to reduce the switching losses. Section III presents the simulation results. Finally section IV gives some conclusions.

II. SAPF CONTROL UNDER UNBALANCED LOAD

A. Unbalanced Tolerant Topology of SAPF

Figure 1 shows the voltage structure of SAPF. This topology is used in industrial applications for their small physical size and the simplicity of their control orders. It is composed by power and control parts.

The power part of this SAPF composed by an output passive filter (R_f, L_f) to filter the high frequency harmonic currents, a power capacitive C for energy storage.

This capacitive ensures a U_{dc} to almost constant value at the input of the inverter and a voltage inverter based on IGBT components. To minimize the harmonics current effects, we have used an unbalanced tolerant shunt SAPF topology (Figure 2). In order to handle the current created by an unbalanced non-linear load, this topology is composed of a conventional three-phase voltage source inverter (VSI).

In first topology(Figure 2(a)), we add a fourth level related to the neutral wire. The fourth level switching is assured by another control based on the current value of neutral wire. In the other and where this fourth level is not available, a second tolerant topology (Figure 2(b)) is used to reduce the neutral current effects. Using this structure, if an unbalanced problem is detected the neutral wire will be connected to the middle point of the U_{dc} .

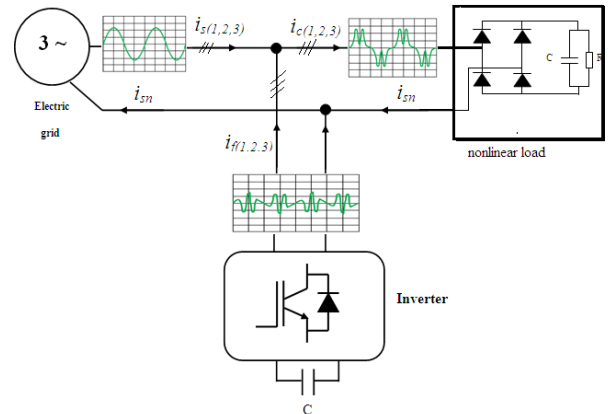


Figure1. General SAPF voltage structure.

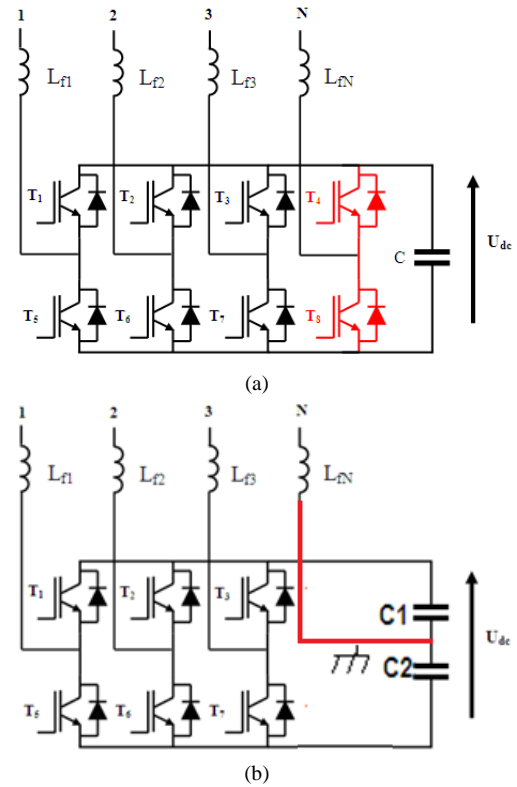


Figure 2. Unbalanced tolerant structure.

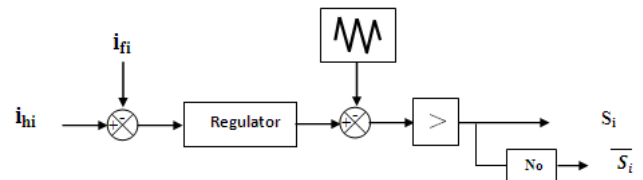


Figure3. Pulse width modulation structure.

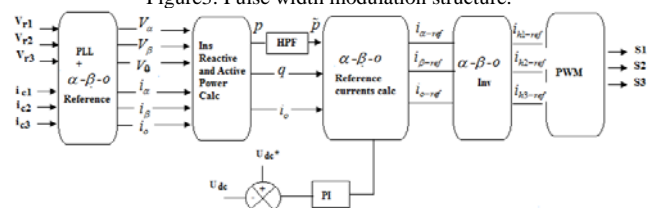


Figure 4. SAPF control circuit diagram.

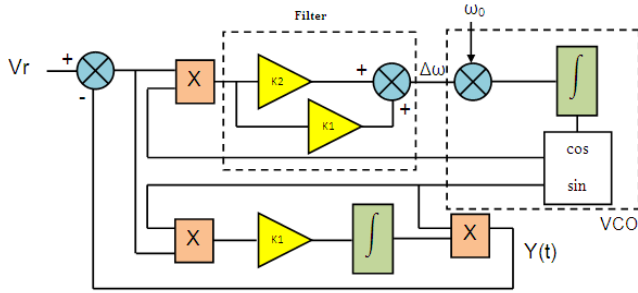


Figure 5. Structure of the PLL technique.

The neutral wire uses an inductance L_{fn} to reduce the current ripple injected. The unbalanced problem is identified with their observed signatures. These signatures are based on the variation of the sum load currents. The algorithm is based on the comparison of the sum of the load current from zero summarized by the two conditions:

$$\begin{aligned} \text{If } i_{c1} + i_{c2} + i_{c3} = 0 &\rightarrow S = 0 \\ \text{If } i_{c1} + i_{c2} + i_{c3} \neq 0 &\rightarrow S = 1 \end{aligned}$$

B. Harmonic Reference Extraction

Using the PWM control strategy, the SAPF tolerant topology allows to eliminate the neutral current i_{sn} and to compensate reactive powers, so to improve the rate current total harmonic distortion (THD). This system can be treated as current sources that compensate in real time the harmonic currents in electric grid with a currents injected by the SAPF and anti-phase to the identified harmonic disturbances.

Figure 4 shows the control strategy of the SAPF. It is based on the identification of harmonic current reference with the instantaneous modified $p-q$ power method with U_{dc} regulation. The main aim of the instantaneous modified $p-q$ power theory is to obtain a constant source power after the compensation with SAPF. The quality of the compensation for harmonic currents highly depends on the performance of the selected identification method [2], [17]. This control is based on the identification of three-phase voltage (V_{r1}, V_{r2}, V_{r3}) with a PLL technique.

Figure 5 shows the overall diagram of a PLL for the harmonics extraction [12], [17], [18]. It is basically a feedback control system that controls the frequency of a voltage controlled oscillator (VCO). The input signal is applied to one of the inputs of a phase detector.

C. Reference Current Signal Generation for SPAF

By using the Clark transformation, we get the following current equations.

$$\begin{bmatrix} i_{\alpha} \\ i_{\beta} \\ i_o \end{bmatrix} = \sqrt{\frac{2}{3}} \begin{bmatrix} 1 & -\frac{1}{2} & -\frac{1}{2} \\ 0 & \frac{\sqrt{3}}{2} & -\frac{\sqrt{3}}{2} \\ \frac{\sqrt{2}}{2} & \frac{\sqrt{2}}{2} & \frac{\sqrt{2}}{2} \end{bmatrix} \begin{bmatrix} i_{c1} \\ i_{c2} \\ i_{c3} \end{bmatrix} \quad (1)$$

The PLL generates the quantities $\sin(\omega t)$ and $\cos(\omega t)$ and then we have the system equations that the voltages (V_{α}, V_{β}) in the stationary reference frame ($\alpha - \beta - o$).

$$V_{\alpha} = \sqrt{3}V_r \sin(\omega t) \quad (2)$$

$$V_{\beta} = -\sqrt{3}V_r \cos(\omega t) \quad (3)$$

The active, reactive and zero-sequence powers are defined as :

$$\begin{bmatrix} p \\ q \\ p_o \end{bmatrix} = \begin{bmatrix} V_{\alpha} & V_{\beta} & 0 \\ -V_{\beta} & V_{\alpha} & 0 \\ 0 & 0 & V_o \end{bmatrix} \begin{bmatrix} i_{\alpha} \\ i_{\beta} \\ i_o \end{bmatrix} \quad (4)$$

The powers in the $\alpha-\beta$ system can be decomposed in mean and alternating values, corresponding to the fundamental and harmonic components.

$$\begin{cases} p = \bar{p} + \tilde{p} \\ q = \bar{q} + \tilde{q} \end{cases} \quad (5)$$

A high pass filter (HPF) shown in Figure 4 is used to separate the alternating of instantaneous active power \tilde{p} and mean value of the instantaneous active power \bar{p} . In order to compensate the reactive power, the instantaneous imaginary power in (4) is set to zero ($q=0$), we obtain :

$$\begin{bmatrix} i_{\alpha-ref} \\ i_{\beta-ref} \end{bmatrix} = \frac{1}{V_{\alpha}^2 + V_{\beta}^2} \begin{bmatrix} V_{\alpha} & V_{\beta} \\ -V_{\beta} & V_{\alpha} \end{bmatrix} \begin{bmatrix} \tilde{p} \\ 0 \end{bmatrix} \quad (6)$$

The zero-sequence instantaneous active power p_o is compensated by using:

$$i_{o-ref} = i_o \quad (7)$$

So we obtain the inverter reference currents:

$$\begin{bmatrix} i_{h1-ref} \\ i_{h2-ref} \\ i_{h3-ref} \end{bmatrix} = \sqrt{\frac{2}{3}} \begin{bmatrix} 1 & -\frac{1}{2} & -\frac{1}{2} \\ 0 & \frac{\sqrt{3}}{2} & -\frac{\sqrt{3}}{2} \\ \frac{\sqrt{2}}{2} & \frac{\sqrt{2}}{2} & \frac{\sqrt{2}}{2} \end{bmatrix} \begin{bmatrix} i_{\alpha-ref} \\ i_{\beta-ref} \\ i_{o-ref} \end{bmatrix} \quad (8)$$

Finally we obtain:

$$i_{hm-ref} = i_{h1-ref} + i_{h2-ref} + i_{h3-ref} \quad (9)$$

The control system (Fig. 4) consists of main blocks:

- Software of PLL
- Determination of $i_{\alpha-ref}$, $i_{\beta-ref}$ and i_{o-ref}
- Calculation of the \tilde{p} , q and p_o powers.

The reference currents in three phase system are calculated in order to compensate neutral, harmonic and reactive currents in the load. The switching signals used in shunt active power filter control algorithm are generated by

comparing reference currents and actual line currents and using PWM current control algorithm (Figure 4).

The inverter input voltage can be calculated as a function of the state of the switch as shown as follow:

$$\begin{bmatrix} V_1 \\ V_2 \\ V_3 \end{bmatrix} = \frac{U_{dc}}{3} \begin{bmatrix} 2 & -1 & -1 \\ -1 & 2 & -1 \\ -1 & -1 & 2 \end{bmatrix} \begin{bmatrix} S_1 \\ S_2 \\ S_3 \end{bmatrix} \quad (10)$$

The state space model of the electric power inverter is:

$$\begin{bmatrix} \frac{di_{f1}}{dt} \\ \frac{di_{f2}}{dt} \\ \frac{di_{f3}}{dt} \end{bmatrix} = \begin{bmatrix} -\frac{R_{f1}}{L_{f1}} & 0 & 0 & \frac{2S_1 - S_2 - S_3}{3L_{f3}} \\ 0 & -\frac{R_{f2}}{L_{f2}} & 0 & \frac{-S_1 + 2S_2 - S_3}{3L_{f3}} \\ 0 & 0 & -\frac{R_{f3}}{L_{f3}} & \frac{-S_1 - S_2 + 2S_3}{3L_{f3}} \end{bmatrix} \begin{bmatrix} i_{f1} \\ i_{f2} \\ i_{f3} \\ U_{dc} \end{bmatrix} - \begin{bmatrix} \frac{V_{r1}}{L_{f1}} \\ \frac{V_{r2}}{L_{f2}} \\ \frac{V_{r3}}{L_{f3}} \end{bmatrix} \quad (11)$$

By using the SPAF equations, the design elements is based on [19]. The use of PWM techniques causes current ripple, that must be kept less than a maximum value ΔI_{max} in order to bound high frequency distortion. The minimum value of inductance L_f is given by :

$$L_f = \frac{U_{dcmax}}{6f_{PWM}\Delta I_{max}} \quad (12)$$

The capacitor value design equation is:

$$C = \frac{2E}{U_{dc0}^2 - U_{min}^2} \quad (13)$$

Where

$$U_{dc0} = \frac{U_{dcmax} + U_{dcmin}}{2} \quad (14)$$

Calculating the value of the capacitor is achieved by fixing the energy stored E and U_{dc0} . The voltage U_{dc} across the capacitor C must be regulated at the reference value. The slow dynamic response of the voltage across the capacitor does not affect the current transient response. Indeed a traditional PI controller represents a simple and effective alternative for the dc-voltage control.

$$K(p) = \frac{K_c}{1 + \tau_c p} \quad (15)$$

To calculate K_c and τ_c , a dc voltage-to-inductor current transfer function is used. The design of this transfer function and the regulator parameters (K_c and τ_c) is detailed in [20]. This paper presents also the design of the PWM PI controller from its transfer function. The PWM technique is based on a comparison between a first signal (modulation signal) and another called carrier signal (triangle wave). The modulation signal is obtained by a current regulator from the error of current signal (Figure 3).

TABLE I. SAPF PARAMETERS

Grid	V_f (RMS)	230 V
	f	50 Hz
	R_s	1 m Ω
	L_s	2 μ H
Non-linear load	R_1	20 Ω
	R_2	40 Ω
	R_3	80 Ω
	$C_1 = C_2 = C_3$	5 mF
	APF	U_{dc}
	$C1=C2$	400 mH
	C	200 mH
	L_f	30 mH
	R_f	0.1 Ω
	f_{PWM}	20KHz
	K_c	0.03
	τ_c	3.6 ms
	L_{on}	10 μ H
	V_f	1 V
	R_{on}	2 m Ω

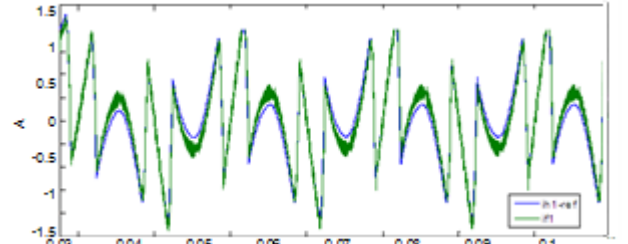


Figure 6. Reference harmonics current pursuit.

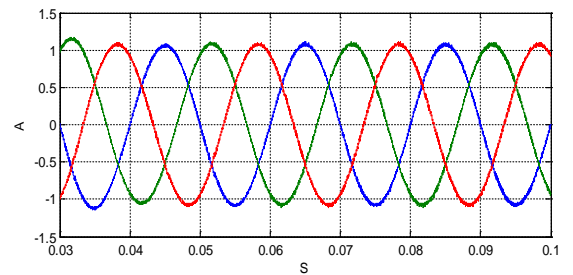


Figure 7. Grid current.

III. SIMULATION RESULTS

To ensure the complete analysis of the SAPF using the voltage inverter, we used the simulation module of Matlab/Simulink. The IGBT component is simulated as a series combination of an inductor L_{on} , small dc voltage source V_f and a resistance R_{on} with an ideal switch controlled. The parameters of the SAPF and IGBT component are listed in Table I.

These parameters are fixed during switching. The objective is to study the operation process of the SAPF in order to verify its performance and to check the waveforms of the currents delivered by the grid.

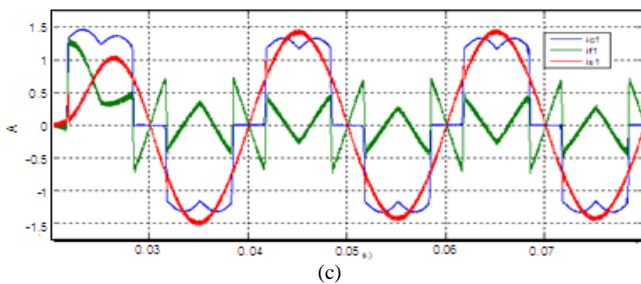
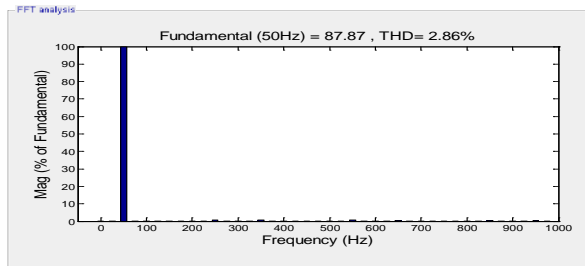
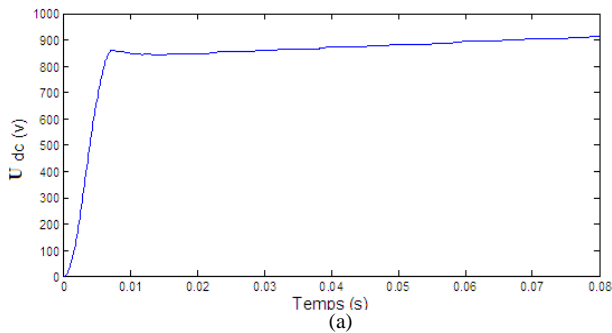


Figure 8. Simulation results with a balanced load.

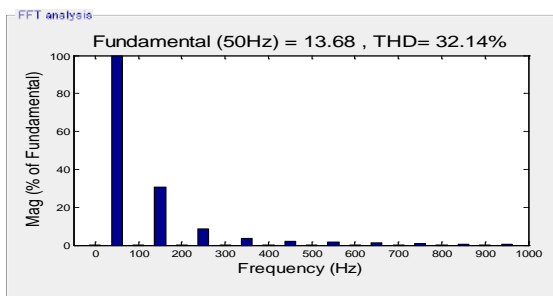
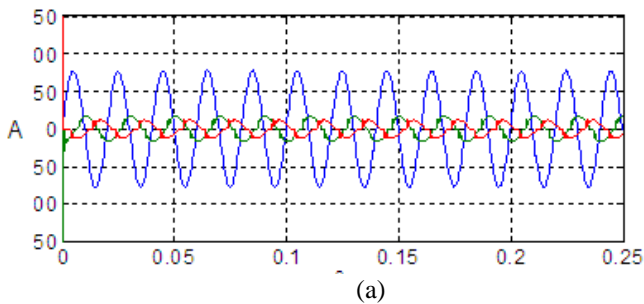


Figure 9. Grid currents waveforms and harmonic spectrum under unbalanced load condition.

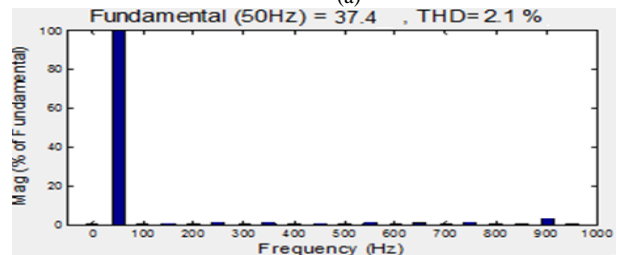
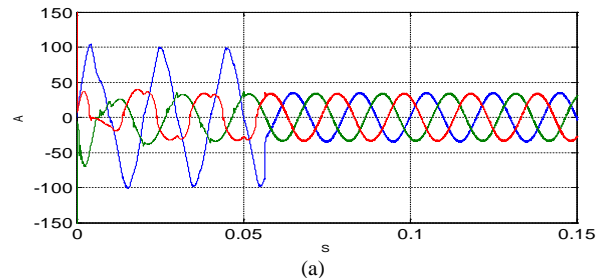


Figure 10. Simulation results for unbalanced load using four leg structure.

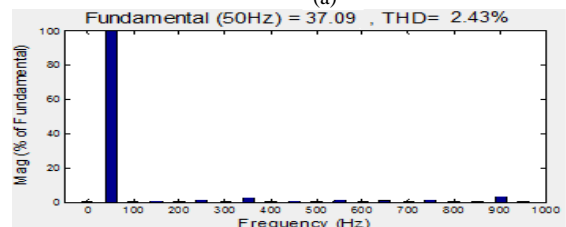
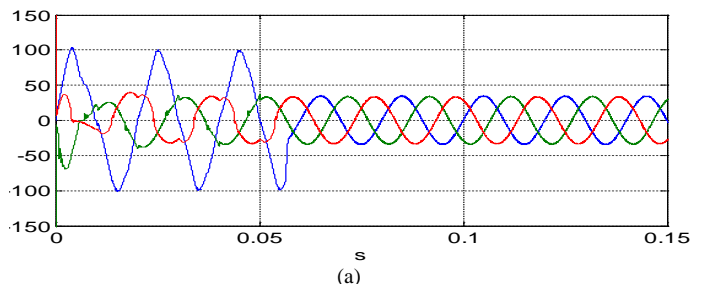


Figure 11. Simulation results for unbalanced load using middle point configuration.

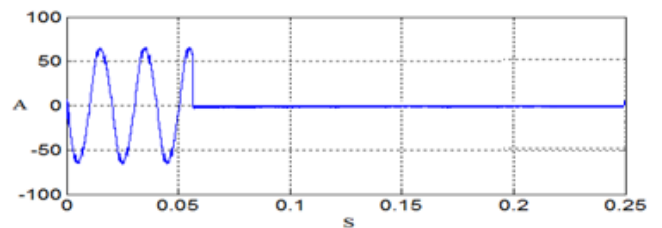


Figure 12. Neural current.

In order to validate the control strategy, a balanced load was first used. By using a three level inverter, the simulation results of the reference harmonic currents identification and pursuit using the p - q power method is shown in Figure 6. The active filter generates a current i_{f1} tracking its reference current i_{h1-ref} .

The Figure 7 indicates that the currents i_{s1} , i_{s2} and i_{s3} issued by the electric grid recover their sinusoidal shape. The current is well depolluted at a fairly satisfactory level. This is

confirmed in Figure 8(a) by the THDi value equal to 2.86%. The Figure 8(b) shows that the DC bus voltage U_{dc} across the capacitor is stabilized at a reference value of 900V. Figure 8(c) shows the wave forms of the i_{c1} , i_{f1} , i_{s1} currents.

By using the same structure and control of SAPF with an unbalanced load, different results are found. In this system, the unbalanced load is based on three single phase diode rectifier. Each single phase diode rectifier is connected to RC circuit. The unbalanced is related to the different values of the resistors R_1 , R_2 and R_3 connected in parallel with identical capacitors C_1 , C_2 and C_3 .

Before filtering, Figure 9(a) shows that the deformation increases the current waves, which causes an increase THD currents harmonic equal to 32.14% shown in Figure 9(b). After filtering, by applying the first tolerant topology (four legs), we obtained an improvement in the shape of current which is supplied by the source. This result is shown in Figure 10(a). The efficiency of this SAPF structure is confirmed by the value of the THDi of first phase which is equal to 2.1% (Figure 10(b)).

The effectiveness of our proposed tolerant controls is confirmed also by the results shown in Figure 11. These results are obtained with the application of the second tolerant structure based on the middle point of U_{dc} . Using this structure, the grid currents are recovered its sinusoidal wave than of healthy mode. This improvement is confirmed also by the first phase THDi value which is equal to 2.43% (Figure 11(b)). After applying of these unbalanced tolerant structures, the magnitude of the neutral current i_{sn} is reduced to a very low value shown in Figure 12 which proves the efficiency of the proposed tolerant structures.

IV. COCLUSION

In this paper, instantaneous $p-q$ active and reactive power tolerant control has been applied to a SAPF to compensate reactive and harmonic currents under balanced and unbalanced load. The SAPF tolerant control based on three phase four wires system is performed. This system is controlled by an instantaneous $p-q$ active and reactive power method to verify its performance. The algorithm used in this application has managed to produce the sinusoidal source current with unity power factor and removing the harmonic contents.

The simulation results presented in this paper confirm the effectiveness of the proposed tolerant control method. These results will be validated and analysed using an experimental setup.

REFERENCES

- [1] K. Steela, and B. Singh Rajpurohit, "A survey on active power filters control strategies," *6th India International Conference on Power Electronics, IEEE*, Dec. 2014, pp. 1–6.
- [2] B. Singh, K. Al Haddad, and A. Chandra, "A review of active filters for power improvement," *IEEE Trans. Ind. Electron.*, vol. 46, no. 5, pp. 960–971, Oct. 2009.
- [3] L. West, "Assessment of and recommendations for RTCA/DO-160F section 22, lightning induced transient susceptibility," *Interaction Note*, Note 618, pp.76–98, April 2001.
- [4] D. R. Dobariya, P. A. Upadhyay, "Simulation and comparison between hybrid active power filter and shunt active power filter," *Intern. Conf. Electrical, Electronics, Signals, Communication and Optimization (EESCO)*, 2015, pp. 1–6.
- [5] S. Karverbar, and D. Patil, "A novel technique for implementation of shunt active power filter under balanced and unbalanced load condition," *International conference on Circuit, Power and Computing Technologies*, Mar. 2013, pp. 1–5.
- [6] N. Duy Dinh, N. Duc Tuyen, G. Fujita, and T. Funabashi, "Adaptive notch filter solution under unbalanced and/or distorted point of common coupling voltage for three-phase four-wire shunt active power filter with sinusoidal utility current strategy," *Generation, Transmission and Distribution, IET*, vol. 9, issue 13, pp. 1580–1596. Jan. 2015.
- [7] T. Hau Vo, M. Liao, T. Liu, Anushree, J. Ravishankar, T. Phung, and J. Fletcher, "Unbalanced power flow analysis in a micro grid," *Intern. Journal of Emerging Technology and Advanced Engineering*, vol. 3, issue 1, pp. 537–541, Jan. 2013.
- [8] H. Hu, W. Shi, Y. Lu, and Y. Xing, "Design Considerations for DSP-controlled 400 Hz shunt active power filter in an aircraft power system," *IEEE Trans. Ind. Electron.*, vol. 59, no. 9, pp. 3624–3634, Sept. 2012.
- [9] S. Biricik, S. Redif, O.C. Ozerdem, and M. Basu "Control of the shunt active power filter under non-ideal grid voltage and unbalanced load conditions," *Power Engineering Conference (UPEC)*, Sept. 2013, pp. 1–5.
- [10] M. Kesler, and E. Özdemir, "Operation of shunt active power filter under unbalanced and distorted load conditions," *Electrical and International Conference on Electrical and Electronics Engineering*, Nov. 2009, pp. 92–96.
- [11] G. A. Dongre, V. V. Choudhari, S. P. Diwan, "A comparison and analysis of control algorithms for Shunt Active Power Filter," *Intern. Conf. Computation of Power, Energy Information and Communication (ICCPEIC)*, 2015, pp. 129–133.
- [12] J. Balcells, M. Lamich, and G. Capella, "LC coupled shunt active power filter (APF): new topology and control method," *International conference Electrical Power Quality and utilisation*, Oct. 2007.
- [13] N. Jain, and A. Gupta, "Comparison between two compensation current control methods of shunt active power filter," *International Journal of Engineering Research and General Science*, vol. 2, issue 5, pp. 603–615, Aug./Sept. 2014.
- [14] A. Eid, M. Abdel-Salam, H. El-Kishk, and T. El-Mohandes "Active power filters for harmonic cancellation in conventional and advanced aircraft electric power systems," *Electric Power Systems Research*, vol. 79, issue 1, pp. 80–88, Jan. 2009.
- [15] J. C. Alfonso-Gil, E. Perez, C. Arino, H. Beltran, "Optimization algorithm for selective compensation in a shunt active power filter," *IEEE Trans. Ind. Electron.*, vol. 62, no. 6, pp. 3351–3361, Jun. 2015.
- [16] R. Panigrahi, B. Subudhi, P.C. Panda, "A Robust LQG Servo Control Strategy of Active Power Filter for Power Quality Enhancement," *IEEE Trans. Ind. Electron.*, vol. 31, no. 4, pp. 373–379, Mar. 2016.
- [17] U. D. Gupta, P. Das, M. A. Hoque, "A fuzzy controlled shunt active power filter for reducing current harmonics and reactive power compensation," *Intern. Conf. Electrical Engineering and Information Communication Technology (ICEEICT)*, 2015, pp. 1–5.
- [18] S. Hirve, K. Chatterjee, B. G. Fernandes, M. Imayavaramban, "PLL-Less active power filter based on one-cycle control for compensating unbalanced loads in three-phase four-wire system," *IEEE Trans. Power Delivery*, vol. 22, no. 4, pp. 2457–2465, Oct. 2007.
- [19] F. Ronchi F., A. Tilli, "Design methodology for shunt active filters," *In 10th International Power Electronics and Motion Control Conference (EPE-PEMC)*, 2002.
- [20] F. Pottker, I. Barbi, "Power factor correction of non-linear loads employing a single phase active power filter: control strategy, design methodology and experimentation," *28th annual IEEE Power Electron. Specialists Conference*, Jun. 1997, pp. 412–417.